Full title: Augmented reality in laparoscopic liver resection evaluated on an ex-vivo animal model with pseudo-tumours

Running head: hepatic resection with augmented reality

Authors: Mourad Abdallah, M.D. (1,2), Yamid Espinel (1), Lilian Calvet, Ph.D. (1,3), Bruno Pereira, Ph.D. (3), Bertrand Le Roy, M.D., Ph.D. (4,1), Adrien Bartoli, Ph.D. (1,3), Emmanuel Buc, M.D., Ph.D. (1,2)

(1) Institut Pascal, UMR6602, Endoscopy and Computer Vision group, Faculté de Médecine, Bâtiment 3C, 28 place Henri Dunant, 63000 Clermont-Ferrand

(2) Department of Digestive and Hepatobiliary Surgery, University Hospital Clermont-Ferrand, 1 Place Lucie et Raymond Aubrac, 63003 Clermont-Ferrand

(3) Biostatistics department (DRCI), University Hospital Clermont-Ferrand, 63000 Clermont-Ferrand

(4) Department of Digestive and Oncologic Surgery, University Hospital Nord St-Etienne, Avenue Albert Raimond 42270 Saint-Priest en Jarez

Corresponding author

Emmanuel Buc, MD, PhD

Department of Digestive and Hepatobiliary Surgery, Estaing Hospital

University of Clermont-Auvergne

1, place Lucie et Raymond Aubrac

63003 Clermont-Ferrand Cedex

Tel: +(33)473752389

Fax: +(33)473750459

Email: ebuc@chu-clermontferrand.fr

Abstract

Background. The aim of this study was to assess the performance of our augmented reality (AR) software (Hepataug) during laparoscopic resection of liver tumours and compare it to standard ultrasonography (US).

Materials and methods. Ninety pseudo-tumours ranging from 10 to 20 mm were created in sheep cadaveric livers by injection of alginate. CT-scans were then performed and 3D models reconstructed using a medical image segmentation software (MITK). The livers were placed in a pelvi-trainer on an inclined plane, approximately perpendicular to the laparoscope. The aim was to obtain free resection margins, as close as possible to 1 cm. Laparoscopic resection was performed using US alone (n=30, US group), AR alone (n=30, AR group) and both US and AR (n=30, ARUS group). R0 resection, maximal margins, minimal margins and mean margins were assessed after histopathologic examination, adjusted to the tumour depth and to a liver zone-wise difficulty level.

Results. The minimal margins were not different between the three groups (8.8, 8.0 and 6.9 mm in the US, AR and ARUS groups respectively). The maximal margins were larger in the US group compared to the AR and ARUS groups after adjustment on depth and zone difficulty (21 vs. 18 mm, p=0.001 and 21 vs. 19.5 mm, p=0.037 respectively). The mean margins, which reflect the variability of the measurements, were larger in the US group than in the ARUS group after adjustment on depth and zone difficulty (15.2 vs. 12.8 mm, p<0.001). When considering only the most difficult zone (difficulty 3), there were more R1/R2 resections in the US group than in the AR+ARUS group (50% vs. 21%, p=0.019).

Conclusion. Laparoscopic liver resection using AR seems to provide more accurate resection margins with less variability than the gold standard US navigation, particularly in difficult to access liver zones with deep tumours.

Key words: laparoscopy, liver, resection, augmented reality, deformable 3D model, overlay

Introduction

Laparoscopic surgery has undergone a rapid development in the recent years. However, despite the improvement of surgical techniques and instruments, as well as the expansion to more complex and risky procedures, some interventions remain very challenging. It is the case of laparoscopic liver resection (LLR). It has clear advantages compared to the open procedure [1,2], namely reduced intraoperative bleeding, hospital stay, post-operative morbidity and narcotic dose requirement, but its use remains limited because of technical issues [3]. These are mainly the control of intraoperative bleeding, which is more difficult in a tighter environment, but also tumour localisation and margin assessment, which are difficult particularly in non-anatomic resections because of the very limited haptic feedback. R1/R2 resection in laparoscopic and open procedures was up to 30% in a recent randomized controlled trail [4], which underlines the limits of intraoperative ultra-sonography (US), knowing that the learning curve of laparoscopic US is much flatter than the one of US in open procedures.

Recently, our team has developed a software called Hepataug, to implement augmented reality (AR), allowing the surgeon to see the subsurface anatomy in a laparoscopic video image [5]. Hepataug works by overlaying the internal anatomical structures obtained from preoperative imagery onto the laparoscopic image. Even though AR was successfully developed for gynaecological, renal, and adrenal surgeries [6–9], and despite considerable research, robust systems capable of handling soft tissue deformations are yet to be created. The state-of-the-art in image-guided surgery for LLR is mostly based on overlaying a rigid preoperative 3D model onto the laparoscopic liver image [10,11]. The extent of modification of the intraoperative organ shape compared to its preoperative shape (hence, its shape as seen in the preoperative imagery) is difficult to assess in liver surgery. Many factors contribute to the organ deformation during laparoscopy, especially cardiopulmonary motion, gas insufflation, and gravity acting in different directions preoperatively and intraoperatively. Partial visibility of the liver during surgery makes the task of correction for the deformations even more challenging.

Our software Hepataug brings a major contribution to image-guided surgery because it uses a deformable preoperative 3D model and works in *de facto* conditions of laparoscopic procedures. We have already evaluated Hepataug quantitatively with *in silico* and phantom experiments [12], and qualitatively with in-vivo laparoscopic images [13]. The results showed that Hepataug is an accurate and faster solution compared to the state-of-the-art. We then demonstrated the feasibility of Hepataug in a clinical situation [14]. However, although Hepataug reveals the precise localisation of the tumours within the liver, especially with isoechogenic tumours non visible with US, its benefits for the quality of the resection remain unclear. Particularly, the accuracy of the resection margins in the oncologic setting was not assessed. In order to further characterise the accuracy and clinical relevance of Hepataug, we now propose to evaluate it extensively, and to compare it with other surgical guidance solutions, in an *ex vivo* animal tumour resection model. The goal of our study was to assess the accuracy of Hepataug against US, which represents the gold standard in intraoperative guidance system. We decided to focus on quantitative margins because the R0/R1 status is a binary status that does not precisely reflect the fine margins of hepatic resection.

Hepataug was created and developed by our research team EnCoV at the University of Clermont Auvergne (UCA), CNRS and CHU Clermont-Ferrand. Hepataug is thus a non-profit research software owned by public research bodies. It has no specific relationships with MITK, which is a free software for 3D liver reconstruction from preoperative data. Concretely, Hepataug uses a 3D model reconstructed from preoperative data, which may be obtained from MITK or any other preoperative reconstruction software, such as 3D Slicer.

Materials and methods

Liver model

We chose the sheep liver as our reference model, as it is macroscopically similar to the human liver, as shown in figure 1. Indeed, it has two separable lobes (and one accessory lobe that can be resected before surgery) with a falciform ligament, and hence possesses the anatomical landmarks required for image augmentation using Hepataug. In addition, its texture and deformability are comparable to the human liver and it has dimensions adapted to perform experiments in a standard pelvi-trainer, where we have conducted the surgical resection in our protocol. Our experiments were performed on fresh cadaveric sheep livers; IRB approval was thus not required.

Creation of a pseudo-tumour

Our protocol was inspired by previous work [15,16]. In order to determine the ideal substance to use, we tested several agents, namely silicon, polyurethane resin and alginate. For each agent, we evaluated the easiness of preparation and injection in the liver parenchyma, the reproducibility, as well as the unwanted visibility of the pseudo-tumour at the liver surface. The goal was to create a substance mixture with an adequate viscosity that would minimise the extravasation from the injection site whilst maintaining a fluidity that permitted the injection through the needle. The goal of this step was to create several tumours within the liver parenchyma ranging from 10 to 20 mm in size. The ideal concentration of the mixture was determined by injecting variable concentrations of the agent in the liver parenchyma. We used ultrasonography during injection in order to control the diffusion of the agent within the liver. The optimal speed and depth of injection were also evaluated during the procedure. Finally, alginate showed the best attributes and was chosen for the creation of the pseudo-tumours. We therefore finalised a special protocol for this agent, as follows. We first added lukewarm water to alginate powder at a concentration of 0.5 g/mL. We then dissolved LMP agarose at a temperature of 65 degrees (Celsius) and added it to the mixture at 37 degrees, to stabilise the preparation and to avoid scattering of the alginate within the liver. Knowing that after 3 minutes the

mixture would reach its semi-solid state and would therefore not be injectable, stirring did not exceeded 60 seconds. The preparation was loaded into a 2 cc syringe. Injection occurred between 1 min 45 seconds and 2 min 30 seconds, on the posterior side of the sheep liver. We created three to five tumours in each liver.

Imaging and creation of a preoperative 3D model

Our goal at this step was to create a virtual preoperative 3D model from imaging. CT scanning appeared to be the optimal morphological exam in order to detect pseudo-tumours in the sheep liver. The lesions appeared to be hyperdense, easily identifiable, with well-defined margins and without intraparenchymal artefacts (see figure 2a). The liver was placed on a rigid surface (see figure 2b). A subcutaneous needle was placed at the origin of the falciform ligament to ease its subsequent localisation in the CT scan. The settings of the machine were adjusted to create a slice thickness of 1.5 mm.

A preoperative 3D model of the sheep liver was then constructed using MITK®, a free medical image segmentation software (see figures 2c and 2d). The segmentation of the liver as well as its inner structures were performed semi-automatically. MITK then created the desired 3D model automatically. This step was followed by smoothing out of the noise and simplification of the 3D model using Meshlab, a mesh processing open source software.

Surgical installation

A pelvi-trainer was installed on the operating table, faced with the laparoscopic screen. The liver was placed on a 45° inclined wooden surface so that its anterior side faced the surgeon, as shown in figure 3a. The liver was therefore positioned almost perpendicularly to the direction of the surgical tools as well as the laparoscope, allowing the surgeon to practice resections on all the segments for a fixed position of the liver, in order to reproduce the clinical situation. The laparoscope was fixed and directed towards the targeted lesion. Laparoscopic scissors and a grasper were placed on both sides

of the camera. All resections were performed using this standard installation and the same port configuration. Facilities for AR and US were placed next to the pelvi-trainer, as shown in figure 3b.

Augmented reality using Hepataug

Hepataug requires the surgeon to choose a still image of the concerned region of the liver. Knowing that during LLR the liver is only partially visible, the resection and image augmentation were performed while visualising only a limited part of the organ. The only constraint imposed by Hepataug is to ensure the visibility of anatomical landmarks used for the image augmentation: the inferior ridge, a part of the upper silhouette, and the falciform ligament junction. Hepataug works semi-automatically. The manual step consists in marking the landmarks on the 3D model and the laparoscopic image (see figures 4a and 4b). Once the registration is done, all the data presented on the 3D model are superimposed on the laparoscopy screen (see figure 4c). Hepataug provides information concerning the lesion's aspect, localisation and depth with the least possible noise. It allows the surgeon to visualise the structures in different dimensions and viewpoints. An optimal tumour resection can therefore be decided.

While experiments advanced, Hepataug was improved. Our team managed to bring into play an important feature: an image of the tumour projection onto the surface of the liver directed along the laparoscope axis. Furthermore, Hepataug was able to grant the surgeon with an improved guidance by showing a ring composed by the projection of the tumour's safe tissue margin onto the liver surface (see figures 5a and 5b). As the laparoscope and the liver are fixed, Hepataug can run continuously during the laparoscopic resection. The augmentation is displayed on the surface to allow the surgeon to cut into the liver whilst respecting the surgical margins, fixed to 1 cm in our model. Information concerning the depth of the tumour are also provided by Hepataug, as shown in the submitted video material.

Surgical resection

The goal of this step was to perform the laparoscopic removal of each pseudo-tumour with a fixed surgical margin of 1 cm, by carrying out a cylindrical resection from the superficial visible part towards the posterior part of the liver. The livers were divided equally and randomly in three groups:

- US group: resection based on laparoscopic ultrasonography (US) and preoperative CT scan (gold standard)

- AR group: resection based on augmented reality with Hepataug solely

- ARUS group: resection based on augmented reality with Hepataug combined with laparoscopic ultrasonography

In each group, eight livers were used, for which thirty pseudo-tumours were created and resected. In the AR group, the procedure started by marking out the safe tissue margin on the liver surface as provided by Hepataug, using the monopolar scissors. It was followed by performing a cylinder-shaped section using cold scissors of the tissue whilst causing the least possible deformation of the liver. In the US group, the CT scan was first analysed to locate the tumours approximately. The surgeon then used an ultrasonography probe to further locate the tumours. Margins of approximately 1 cm were marked around the lesion followed by the surgical procedure. In the ARUS group, we started by localising the tumour using AR. After marking the resection limits on the liver surface, ultrasonography was used to verify if a 1 cm margin was respected before and during the surgical removal of the tumour.

Knowing that the sheep liver is not homogenous and that surgical obstacles can change depending on the lesion location and depth, the organ was divided in three zones representing the multiple difficulty levels of liver resection (see figure 6). This classification was based on three criteria: parenchyma thickness, degrees of difficulty met during the training sessions, and the angle formed by the surgical instrument with the liver surface (an excision of the parenchyma performed with a 90° angle is easier, because of navigation in a lesser parenchyma thickness and therefore a lesser risk of error concerning the resection path). The three proposed difficulty zones are:

- Zone 1: thin liver tissue, with laparoscope almost perpendicular to the resection plane;

- Zone 2: medium liver thickness or thin tissue with laparoscope non-perpendicular to the resection plane;

- Zone 3: thick liver tissue with an acute angle of resection.

Pathological analysis

The specimen was sectioned with a scalpel horizontally. Knowing that we opted for cylindrical resections, margins regarding the superficial and deep sides were not explored. The smallest surgical margin was analysed macroscopically after staining the sections with toluidine blue. It was then removed from the specimen, fixed and transported in formalin 4%. Two days later, the specimens were embedded in paraffin and sectioned with a microtome in order to obtain 5 micrometres sections for microscopical evaluation. A positive margin (R1 or R2) was defined by tumour abutment of the enucleation capsule.

Endpoints

For each lesion the following data were collected: dimensions of the tumour along the three axes, volume, depth, difficulty zone, minimal and maximal resection margins in millimetres. The endpoints were R0 (margin $\geqslant$ 1 mm) vs R1 (margin < 1 mm) resection, minimal and maximal resection margins and the average margin (defined as the average between minimal and maximal margins, which reflects the variability of the measurements). A comparison was made between the three groups (US, AR and ARUS) and after pooling AR and ARUS, as resection margins were drawn using AR in these two groups.

Statistical analyses

Continuous data were expressed, according to the statistical distribution, as mean and standard deviation. To account for the between- and within-liver variability caused by several measurements

being taken for the same liver, random-effects models for the tumours correlated data (linear for continuous dependent endpoint and generalized linear for categorical endpoint) were used to compare the three groups. Indeed, due to the falsified assumption of independence, these models were preferred over the usual statistical tests specific to independent data. The normality of the residuals from linear models was studied using the Shapiro-Wilk test. When appropriate, the data were log-transformed to achieve normality of the dependent endpoint. Multivariable analysis was conducted to take into account adjustment on the following confounders variables: tumour depth and zone difficulty. The statistical analyses were performed using the Stata software version 15 (StataCorp, College Station, US). The tests were two-sided with the type-I error set at 5%. The Sidak post hoc test was applied to correct the type-I error due to multiple comparisons.

Results

Among 151 tumours created in 22 livers, 32 were not segmented because of unexpected visibility of the tumour at the liver surface (n=5), intra-parenchymal scattering (n=21) or non-spherical aspect of the lesion (n=6). A total of 29 pseudo-tumours were used for the development and tuning of the protocol – optimisation of Hepataug, improvement of the visualisation and standardisation of the surgical technique. Finally, 90 tumours were surgically resected: 30 in the US group, 30 in the AR group and 30 in the ARUS group. The average number of tumours in each difficulty zone was not different between the three groups (see table 1). In contrast, tumour volumes as well as tumour depth were lower in the US group.

The mean minimal resection margins were 8.8 ± 4.2 mm, 8.0 ± 3.4 mm and 6.9 ± 3.2 mm in the US, AR and ARUS groups respectively (see table 2). This was not statistically different in univariate analysis (p=0.49 between US and AR, p=0.08 between US and ARUS and p=0.29 between AR and ARUS) and after adjustment on depth and zone difficulty (p=0.57 between US and AR, p=0.13 between US and ARUS and p=0.35 between AR and ARUS). After pooling the groups AR and ARUS, the minimal margins remained non statistically different, even after adjustment on depth and zone difficulty (8.8 ± 4.2 vs. 7.5 ± 3.3 mm, p=0.23) (see table 3).

The mean maximal resection margins were 21.6 ± 4.7 mm, 20.0 ± 3.6 mm and 18.6 ± 4.2 mm in the US, AR and ARUS groups respectively (see table 2). The difference was significant only between US and ARUS (p=0.005). After adjustment to tumour depth and zone difficulty, the maximal margins were higher in the US group compared to both the AR and the ARUS groups with statistically significant results (p=0.001 and p=0.037 respectively). After pooling the groups AR and ARUS, the maximal margins were significantly higher in the US group (21.6 ± 4.7 vs. 19.3 ± 4.0 mm for the AR+ARUS group, p=0.015) particularly after adjustment on tumour depth (p=0.002), zone difficulty (p=0.005) and both (p=0.002) (see table 3).

The mean average margins were respectively of 15.2 ± 2.7, 14.0 ± 2.5 and 12.8 ± 2.6 mm in the US, AR and ARUS groups. The difference was significant only between US and ARUS (p=0.001) (table 2). After adjustment on tumour depth and zone difficulty, the difference remained statistically significant only between US and ARUS (p<0.001) but tended to reach significance between US and AR (p=0.064). After pooling the groups AR and ARUS, the average margins were significantly larger in the US group (15.2 ± 2.7 vs. 13.4 ± 2.6 mm, p=0.01), particularly after adjustment on tumour depth (p=0.01), zone difficulty (p=0.003) or both (p=0.004) (table 3). Concerning specifically the ARUS group, the resection margins were first drawn using the AR projection of the margins at the liver surface, and US was used thereafter for resection guidance. In this case only 9 resections (30%) were influenced by US, because of the risk of resection margins inferior to 1 cm.

There were no statistical difference in R0 resection between the three groups, even after pooling the groups AR and ARUS (p=0.34) and after adjustment on depth (p=0.25) and difficulty zone (p=0.26) (see table 2). The rate of R1/R2 resections was 13.3%, 6.7% and 6.7% in the US group, AR group and ARUS group respectively. This was not statistically different in univariate analysis (p=0.42 between US and AR, 0.42 between US and ARUS and 0.98 between AR and ARUS), even after adjustment on depth and zone difficulty (p=0.17 between US and AR, p=0.26 between US and ARUS and p=0.36 between AR and ARUS). After pooling the groups AR and ARUS, R1/R2 resections remained non statistically different even after adjustment on depth and zone difficulty (13.3% vs. 6.7%, p=0.24). However, when considering only the zone of difficulty 3, there were more R1/R2 resections in the US group than in the AR+ARUS group (50% vs. 21%), which was statistically significant after adjustment on tumour depth (p=0.019) (see table 3).

Discussion

Our results are promising. Hepataug proved to be more efficient than ultrasonography, as only 2 R1/R2 resections were observed in groups AR or ARUS compared to 5 R1/R2 resections in the US group. This trend became significant in difficult resections (zone 3) after adjustment on tumour depth (3/14, 21% vs. 3/6, 50% respectively, p=0.019). This rate of R1/R2 resection could be interpreted as very high in our study, especially as resections were performed in thin livers with small tumours. However, the margins in hepatic laparoscopic surgery have been assessed prospectively in a randomized controlled trial, and showed a 28% rate of R1/R2 resections (the OSLO-COMET trial). This is higher than our global results (13.3% in the US group) and similar to our worse results (between 21 and 50% for deep and difficult resections). Furthermore, this trial included patients not only with anatomic resections but also with non-anatomic resections, which usually show lower rate of R1/R2 resections. In addition, the experimental conditions of our study in the pelvi-trainer may have worsen the margins, because of surgical ergonomic being impaired compared to live surgical conditions. It is essential to insist on the fact that our resection using AR does not depend on a special mental effort or reasoning of the surgeon on the virtual 3D representation. The surgical enucleations were performed according to Hepataug's recommendations. The liver incision was done in the same direction all along the parenchymal transection. In contrast, using US alone requires meticulous analysis of the preoperative CT scan. Knowing that the US image is in 2D, the surgeon has to create a mental representation of the pseudo-tumour in a 3D space, based on the visualised image and the preoperative CT scan, and to adapt the resection plane during transection. Furthermore, it is difficult to maintain accurately the axial probe of the US perpendicular to the liver surface, especially in the case of deep tumours or lesions located in the posterior segments. Thus, adequate surgical resection requires important mental efforts from the surgeon and forms a source of imprecision. This seems to be well-illustrated by our experiments, as a larger number of R1/R2 type resections were observed using US alone, especially in the regions where surgery had higher difficulty rates (zone 3, deep tumours). It is interesting to note that the mean minimal margins in the US group were larger (8.8

mm) compared to AR (8.0 mm) and ARUS (6.9 mm), even if non statistically significant. One could conclude that US can improve oncologic margins compared to AR. However, unfavourable tumour features were associated with AR in our study: both the volume and the depth of the tumours in the AR group (with or without US) appeared to be significantly higher compared to the US group, with therefore a higher risk of R1 resection. Furthermore, the maximal margins were larger using US compared with AR and ARUS, with statistically significant results after adjustment on tumour depth and zone difficulty (US vs. AR: 21 vs. 18 mm p=0.001; US vs. ARUS: 21 vs 19.5 mm p=0.034). These results could elucidate the fact that, while using US, surgeons tend to resect larger parenchyma volumes around the tumours in order to ensure negative margins on the pathologic analysis, because US is less accurate than AR. This lack of accuracy of US is revealed by its higher variability in the quality of resection margins compared to AR, as shown by the average margins being significantly closer to 1 cm in groups using AR (the AR and ARUS groups).

Concerning the ARUS group, when US was performed before AR, the limits of the resection at the liver surface were often inconsistent with AR, which was related to the position of the US probe on the liver surface, which is very operator dependent. We then decided to perform AR first, and to use US afterwards, to check the resection margins imposed by AR. Modifications during the resection based on US were done because of a risk of resection with insufficient margins (inferior to 1 cm). It is important to mention that only 9 resections (30%) were influenced by US, keeping in mind that margins calculation using a 2D image is very subjective. Then, as AR was slightly modified by US in the ARUS group, we decided to perform a supplementary analysis between the three groups after pooling the AR and ARUS groups, in order to improve the comparison between the US and AR groups.

The literature concerning image-guided liver surgery remains limited, despite the rapid development of such systems in the recent years. Several teams have developed software, which are all research software, hence not yet publicly available. Many still lack precision [10,11,17–19], because they do not compensate for the liver deformation or because they do not exploit all the available anatomical

landmarks to resolve the deformation. Luo et al. reported another AR system for laparoscopic liver resection [20]. The two systems are substantially different, both from a hardware and a software standpoints. In terms of hardware, Luo et al.'s system was designed specifically for 3D laparoscopes, and requires an optical tracking device to be introduced in the operating theatre; in contrast, Hepataug works with any laparoscope, both regular 2D and 3D ones. In terms of software, Luo et al.'s system uses several steps to solve the preoperative to intraoperative registration problem, involving deep learning to perform intraoperative 3D reconstruction and the well-known Iterative Closest Point (ICP) algorithm; in contrast, Hepataug solves registration directly from the laparoscopic images with a custom-made algorithm. Lastly, in terms of performance, Luo et al. have reported reprojection errors in the range of 6 to 8 mm, which is on par with what Hepataug achieves. We point out that the reprojection error is different from the target registration error (TRE), which would be the important measure to evaluate for quantifying a system's performance, but which cannot be directly evaluated owing to the lack of ground-truth observations of internal organ structures. In short, Luo et al.'s system and Hepataug are substantially different, the latter having a strong advantage over the former owing to its compatibility with any existing laparoscopic device. Hepataug has other multiple advantages compared to its competitors. Firstly, it was created specifically for use during laparoscopic monocular liver surgery. Secondly, it requires the presence of a simple PC in the operating room. Any hospital personnel with medical background can perform the necessary tasks for liver registration. Finally, the intraoperative habits of the medical and paramedical workers remain unchanged while using Hepataug, especially concerning the operating time. One of the main progresses our team made during the proposed experiments was to develop a visualisation module for the 3D image of the tumour projected on the liver surface. Hepataug also has the capacity to provide the surgeon with information concerning the access points on the liver surface adapted to the chosen requested margins. It exposes at the same time data regarding the direction of the desired resection, as well as tumour depth. It is important to mention that Hepataug, and AR in general, can be particularly useful for

tumourectomy (*i.e.*, non-anatomic resection), as resection is guided by the tumour itself, and not by specific anatomic landmarks as in anatomic resection.

Hepataug has limits. The preoperative phase is time-consuming, due to the absence of automatic organ segmentation technique. Intraoperative image registration only works for a static image, or, as in the proposed experiment, for a fixed camera and liver. Despite recent advances in accuracy and usability, our team has not managed yet to implement image-based liver tracking and image fusion in real-time. The latter would allow one to compute the camera motion from a motion picture and therefore to create the augmentation at the physically correct location in spite of camera movements and organ mobilisation. This is currently the subject of fundamental research in our group and will be based on classical computer vision and modern deep learning techniques. However, any further development of Hepataug is not sensible before its precision in localising the liver's inner structures such as tumours be thoroughly evaluated. This is precisely the objective of our experiments in this study on *ex-vivo* sheep livers. In order to quantify the capability and usability of Hepataug, it was necessary to compare it to the gold standard system of image-guided surgery provided by intraoperative ultrasonography combined with the visual inspection of the preoperative CT scan. It is important to mention that our study does not evaluate the capacity of Hepataug to adequately reveal information about the positioning of tumours relatively to other intra-parenchymal structures such as vessels. It is evident that this task requires experiments with *in-vivo* animal models, which require a liver tracking technology to be first developed.

Conclusion

Our experiments bring attention to the benefits of AR guidance during laparoscopic liver surgery. AR provides accurate and objective data to the surgeon and therefore has the potential to reduce surgical errors. In the near future, Hepataug will be able to track the liver deformations in real-time and to visualise the relations between the intra-parenchymal lesions and the major structures such as the vessels. This study represents the first quantitative evaluation of any AR guidance system in liver surgery at this scale.

Disclosures:

Mourad Adballah: no conflict of interest

Yamid Espinel: no conflict of interest

Lilian Calvet: no conflict of interest

Bruno Pereira: no conflict of interest

Bertrand Le Roy: no conflict of interest

Adrien Bartoli: no conflict of interest

Emmanuel Buc: no conflict of interest

References

1. Slakey DP, Simms E, Drew B, Yazdi F, Roberts B (2013) Complications of liver resection: laparoscopic versus open procedures. JSLS 17:46–55 . https://doi.org/10.4293/108680812X13517013317716

2. Landi F, De' Angelis N, Scatton O, Vidal X, Ayav A, Muscari F, Dokmak S, Torzilli G, Demartines N, Soubrane O, Cherqui D, Hardwigsen J, Laurent A (2017) Short-term outcomes of laparoscopic vs. open liver resection for hepatocellular adenoma: a multicenter propensity score adjustment analysis by the AFC-HCA-2013 study group. Surg Endosc 31:4136–4144 . https://doi.org/10.1007/s00464-017-5466-4

3. Goumard C, Farges O, Laurent A, Cherqui D, Soubrane O, Gayet B, Pessaux P, Pruvot F-R, Scatton O, French Association for Hepatobiliary and Pancreatic Surgery (2015) An update on laparoscopic liver resection: The French Hepato-Bilio-Pancreatic Surgery Association statement. J Visc Surg 152:107–112 . https://doi.org/10.1016/j.jviscsurg.2015.02.003

4. Fretland ÅA, Dagenborg VJ, Bjørnelv GMW, Kazaryan AM, Kristiansen R, Fagerland MW, Hausken J, Tønnessen TI, Abildgaard A, Barkhatov L, Yaqub S, Røsok BI, Bjørnbeth BA, Andersen MH, Flatmark K, Aas E, Edwin B (2018) Laparoscopic Versus Open Resection for Colorectal Liver Metastases: The OSLO-COMET Randomized Controlled Trial. Ann Surg 267:199–207 . https://doi.org/10.1097/SLA.0000000000002353

5. Phutane P, Buc E, Poirot K, Ozgur E, Pezet D, Bartoli A, Le Roy B (2018) Preliminary trial of augmented reality performed on a laparoscopic left hepatectomy. Surg Endosc 32:514–515 . https://doi.org/10.1007/s00464-017-5733-4

6. Su L-M, Vagvolgyi BP, Agarwal R, Reiley CE, Taylor RH, Hager GD (2009) Augmented reality during robot-assisted laparoscopic partial nephrectomy: toward real-time 3D-CT to stereoscopic video registration. Urology 73:896–900 . https://doi.org/10.1016/j.urology.2008.11.040

7. Bourdel N, Collins T, Pizarro D, Debize C, Grémeau A-S, Bartoli A, Canis M (2017) Use of augmented reality in laparoscopic gynecology to visualize myomas. Fertil Steril 107:737–739 . https://doi.org/10.1016/j.fertnstert.2016.12.016

8. Collins T, Pizarro D, Bartoli A, Bourdel N, Canis M (2014) Computer-aided laparoscopic myomectomy by augmenting the uterus with pre-operative MRI data. ISMAR - IEEE International Symposium on Mixed and Augmented Reality

9. Ieiri S, Uemura M, Konishi K, Souzaki R, Nagao Y, Tsutsumi N, Akahoshi T, Ohuchida K, Ohdaira T, Tomikawa M, Tanoue K, Hashizume M, Taguchi T (2012) Augmented reality navigation system for laparoscopic splenectomy in children based on preoperative CT image using optical tracking device. Pediatr Surg Int 28:341–346 . https://doi.org/10.1007/s00383-011-3034-x

10. Soler L, Nicolau S, Pessaux P, Mutter D, Marescaux J (2014) Real-time 3D image reconstruction guidance in liver resection surgery. Hepatobiliary Surg Nutr 3:73–81 . https://doi.org/10.3978/j.issn.2304-3881.2014.02.03

11. Ntourakis D, Memeo R, Soler L, Marescaux J, Mutter D, Pessaux P (2016) Augmented Reality Guidance for the Resection of Missing Colorectal Liver Metastases: An Initial Experience. World J Surg 40:419–426 . https://doi.org/10.1007/s00268-015-3229-8

12. Özgür E, Koo B, Le Roy B, Buc E, Bartoli A (2018) Preoperative liver registration for augmented monocular laparoscopy using backward-forward biomechanical simulation. Int J Comput Assist Radiol Surg 13:1629–1640 . https://doi.org/10.1007/s11548-018-1842-3

13. Le Roy B, Ozgur E, Koo B, Buc E, Bartoli A (2019) Augmented reality guidance in laparoscopic hepatectomy with deformable semi-automatic computed tomography alignment (with video). J Visc Surg 156:261–262 . https://doi.org/10.1016/j.jviscsurg.2019.01.009

14. Le Roy B, Abdallah M, Espinel Y, Calvet L, Pereira B, Ozgur E, Pezet D, Buc E, Bartoli A (2020) A case series study of augmented reality in laparoscopic liver resection with a deformable preoperative model. Surg Endosc 34:5642–5648 . https://doi.org/10.1007/s00464-020-07815-x

15. Chauvet P, Collins T, Debize C, Novais-Gameiro L, Pereira B, Bartoli A, Canis M, Bourdel N (2018) Augmented reality in a tumor resection model. Surg Endosc 32:1192–1201 . https://doi.org/10.1007/s00464-017-5791-7

16. Chabrot P (2016) Modèle de simulation en radiologie. 5ème colloque francophone de simulation en santé

17. Schneider C, Thompson S, Totz J, Song Y, Allam M, Sodergren MH, Desjardins AE, Barratt D, Ourselin S, Gurusamy K, Stoyanov D, Clarkson MJ, Hawkes DJ, Davidson BR (2020) Comparison of manual and semi-automatic registration in augmented reality image-guided liver surgery: a clinical feasibility study. Surg Endosc 34:4702–4711 . https://doi.org/10.1007/s00464-020-07807-x

18. Golse N, Petit A, Lewin M, Vibert E, Cotin S (2020) Augmented Reality during Open Liver Surgery Using a Markerless Non-rigid Registration System. J Gastrointest Surg. https://doi.org/10.1007/s11605-020-04519-4

19. Lau LW, Liu X, Plishker W, Sharma K, Shekhar R, Kane TD (2019) Laparoscopic Liver Resection with Augmented Reality: A Preclinical Experience. J Laparoendosc Adv Surg Tech A 29:88–93 . https://doi.org/10.1089/lap.2018.0183

20. Luo H, Yin D, Zhang S, Xiao D, He B, Meng F, Zhang Y, Cai W, He S, Zhang W, Hu Q, Guo H, Liang S, Zhou S, Liu S, Sun L, Guo X, Fang C, Liu L, Jia F (2020) Augmented reality navigation for liver resection with a stereoscopic laparoscope. Comput Methods Programs Biomed 187:105099 . https://doi.org/10.1016/j.cmpb.2019.105099
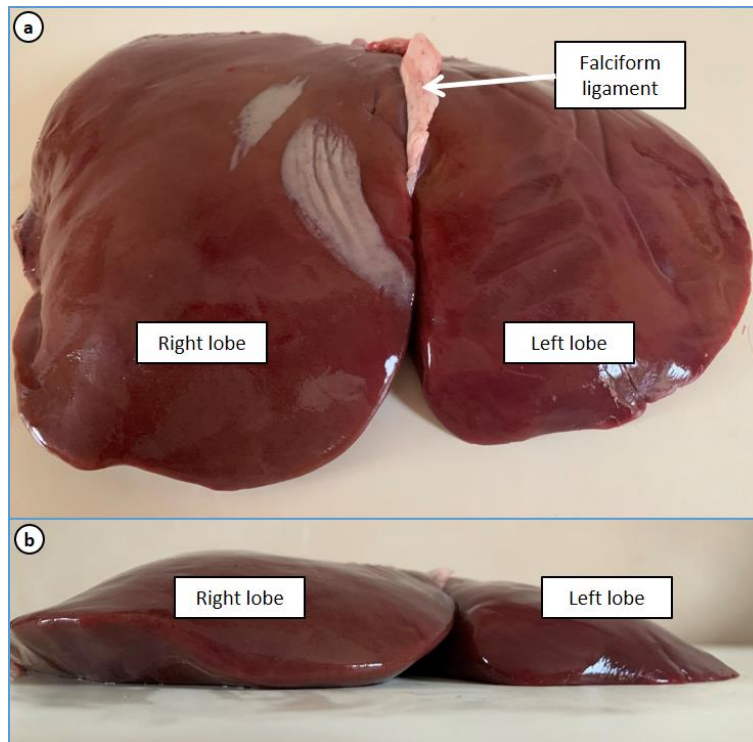
Figure 1: Photography of an *ex-vivo* sheep liver. a) anterior view, showing the falciform ligament dividing the liver in two distinct lobes, as in the human liver; b) inferior view, showing that sheep livers are very thin compared to human livers.
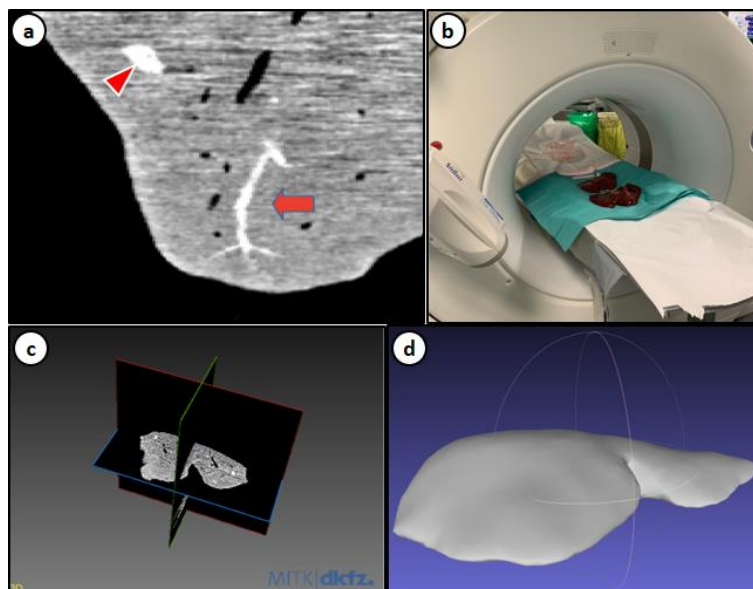
Figure 2: Imaging of the 3D model. a) CT visualisation of the pseudo-tumour (red arrowhead) and an hepatic vein (red arrow); b) sheep liver within the CT-scanner; c) sheep liver after slicing; d) reconstruction of a virtual preoperative 3D model using the free medical imaging reconstruction software MITK.
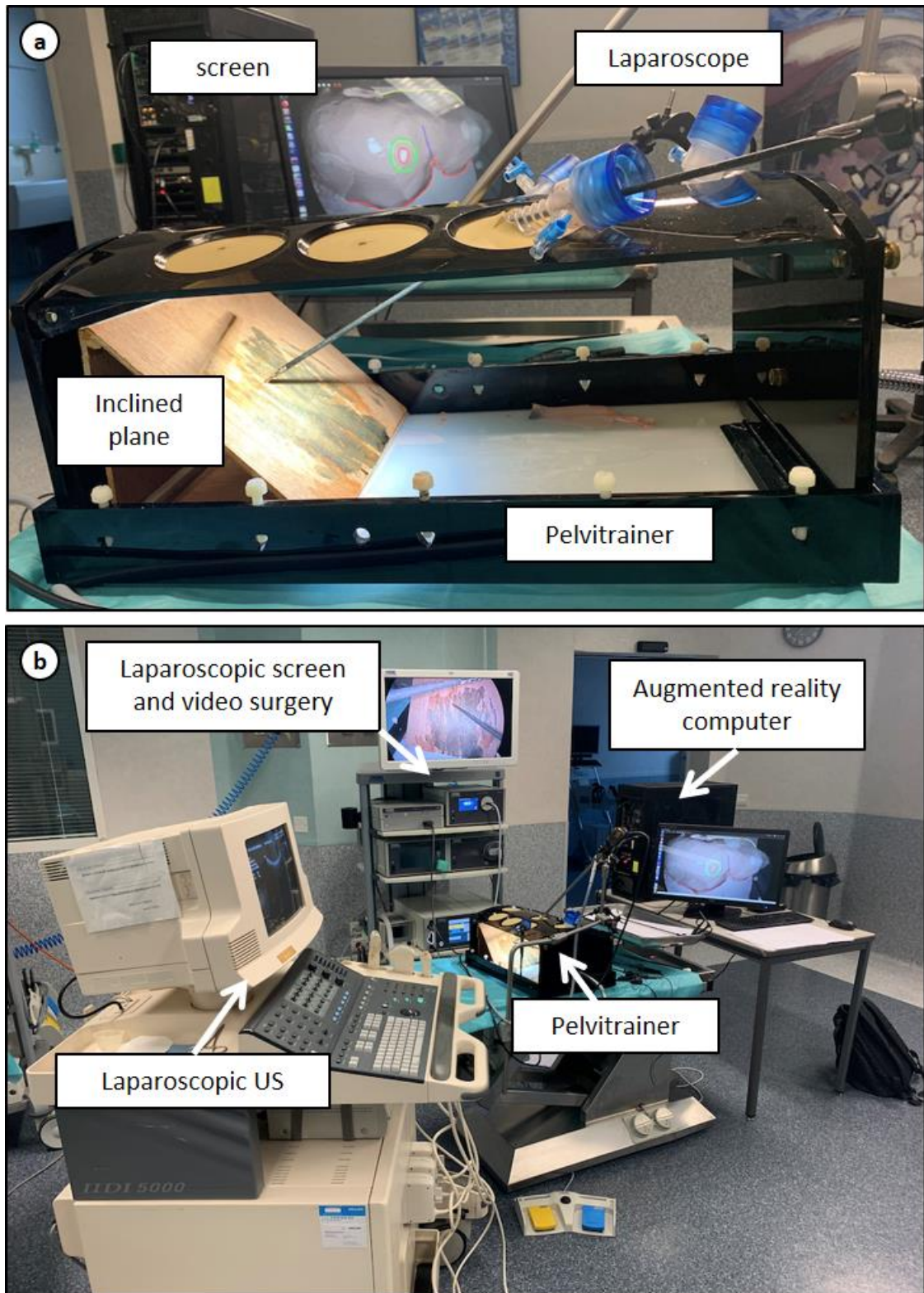
Figure 3: Surgical setup for the resection of the tumours. a) view of the pelvi-trainer with the inclined wooden plane and the perpendicular axis of the laparoscope; b) overview of the operating room with the laparoscopic US and the AR devices.
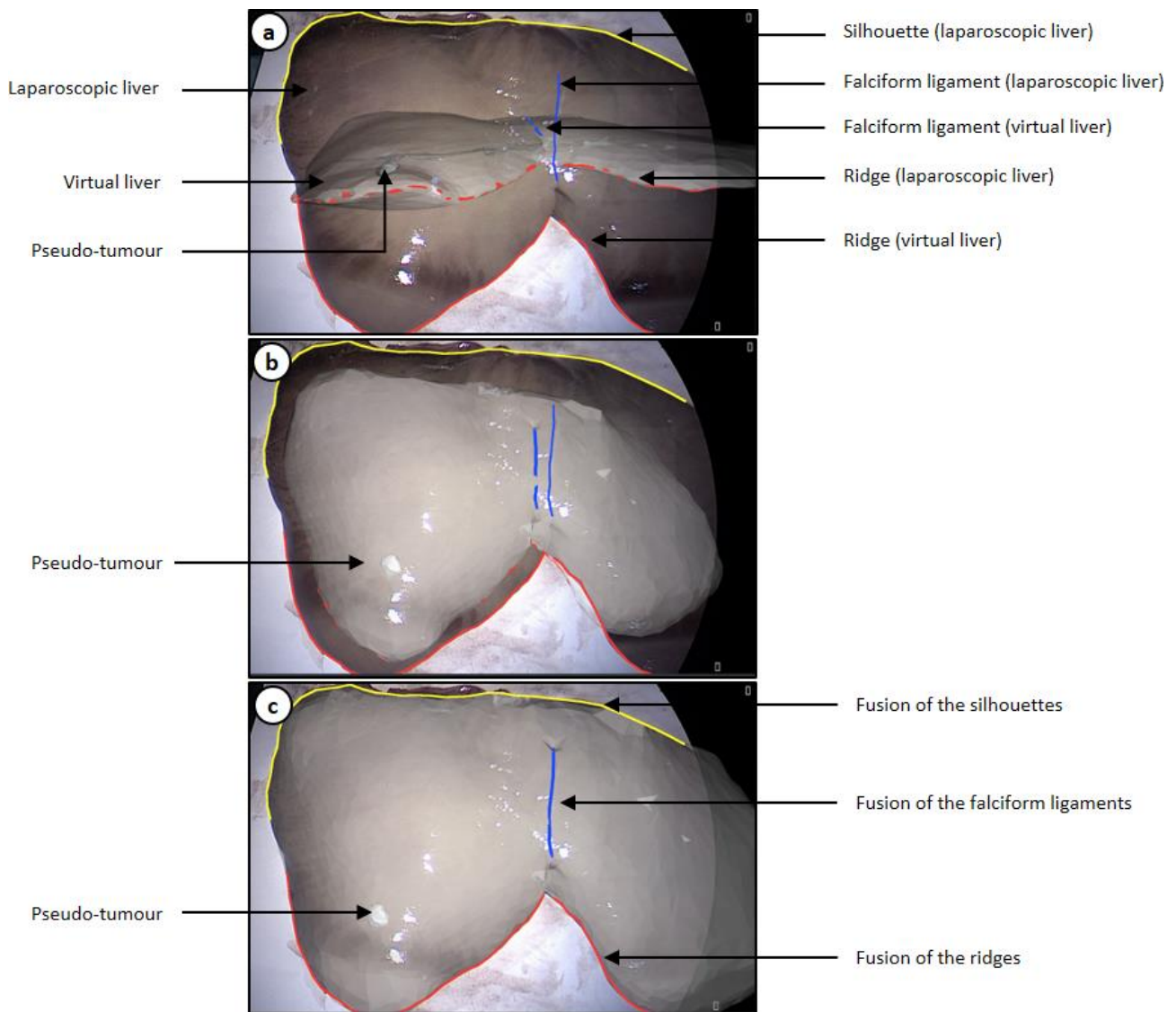
Figure 4: Augmented reality using Hepataug. a) after screenshot of the laparoscopic screen, the ridge (red line), the silhouette (yellow line), and the falciform ligament (blue line) are drawn on the laparoscopic image (continuous lines) and on the 3D model (dotted lines); b) 3D model and real liver before the beginning of the procedure; c) Hepataug runs and the 3D model is superimposed on the laparoscopic screen.
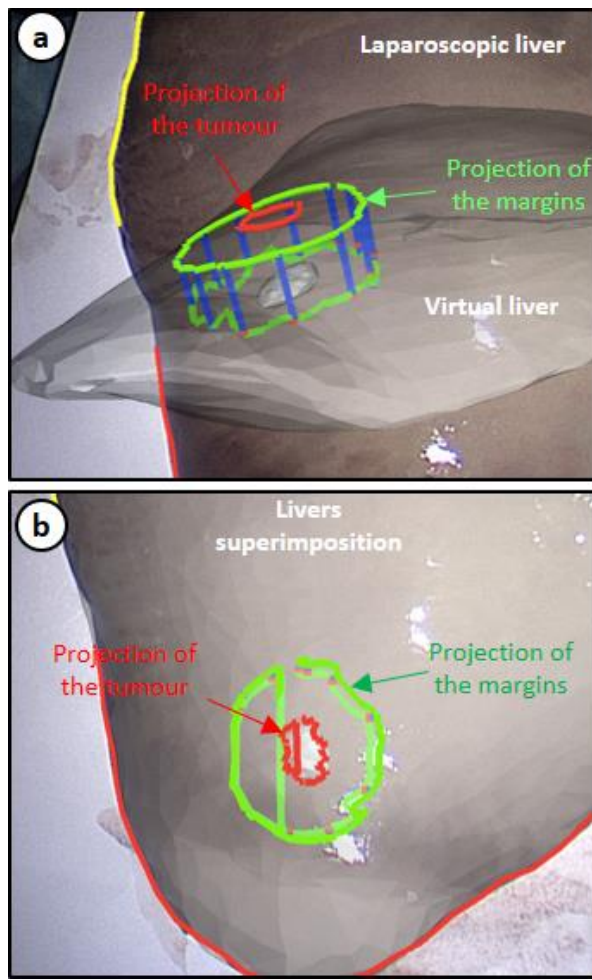
Figure 5: Preoperative 3D model of the liver with compensated deformation, with projection of the tumour (red line) and the 1 cm peri-tumoural margins (green line) onto the liver surface. a) before augmented reality, the blue lines are disposed every 1 cm as a gradual scale ; b) following augmented reality, the resection margins are in the same axis as the laparoscope to facilitate the resection.
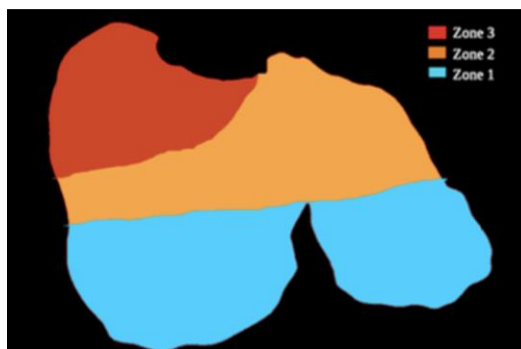
Figure 6: Segmentation of the liver in 3 difficulty zones: zone 1 is for thin liver tissue with the laparoscope almost perpendicular to the resection plane; zone 2 is for medium thickness or thin tissue with laparoscope non-perpendicular to the resection plane; zone 3 is for thick tissue with an acute angle of resection.